

# Molecular beam photoelectron spectroscopy of SO<sub>2</sub>: Geometry, spectroscopy, and dynamics of SO<sub>2</sub><sup>+</sup>

Laisheng Wang, Y. T. Lee, and D. A. Shirley

Materials and Chemical Sciences Division, Lawrence Berkeley Laboratory and Department of Chemistry, University of California, Berkeley, California 94720

(Received 15 December 1986; accepted 18 May 1987)

We have reinvestigated the He I (584 Å) photoelectron spectroscopy of SO<sub>2</sub> using a supersonic molecular beam. High resolution and rotational cooling allowed us to observe new features and to resolve explicitly the vibrational structure in the first six electronic states of SO<sub>2</sub><sup>+</sup> ion. Improved spectroscopic constants for the ionic states and the adiabatic ionization potentials (IPs) are reported. The vibrational structure of the transition to the  $\tilde{X}^2A_1$  ground state was assigned to the  $\nu_2$  mode exclusively. Irregularity of the vibrational progression on the high IP side was observed, which indicated a potential barrier (to linearity) along the direction of  $Q_2$  coordinate. The barrier height was estimated to be 0.42 eV (3400 cm<sup>-1</sup>). Unusual vibrational structure in the  $\tilde{A}^2A_2$  state was observed, due to the principal excitation of the  $\nu_3$  mode and the presence of a potential barrier along the  $Q_3$  coordinate. The barrier height was estimated to be less than 220 cm<sup>-1</sup>. A new progression was resolved in the  $\tilde{B}^2B_2$  state, which was assigned to be a combination of  $\nu_2$  with  $2\nu_3$ . The  $\nu_2$  vibration was observed to be strongly coupled with the  $\nu_3$  mode. The dynamics of the ion dissociations in the  $\tilde{C}$ ,  $\tilde{D}$ , and  $\tilde{E}$  states was discussed in connection with previous works. A satellite band at about 17.5 eV with resolved vibrational structure which consists of two  $\nu_1$  vibrational progressions was observed.

## I. INTRODUCTION

Many experimental methods have been used to study molecular ions, because of their important role in atmospheric chemistry and physics.<sup>1</sup> Molecular photoelectron spectroscopy (PES) is intrinsically concerned with the properties and spectroscopy of molecular ions, and PES has contributed a great deal to our knowledge of these ions. Although rotationally resolved PES is only possible for the lightest diatomic molecules with a conventional photon source (He I, 584 Å),<sup>2</sup> sufficiently high resolution PES can still provide substantial information about the energy levels, geometries, and dynamics of the molecular ions.<sup>3</sup> The non-resonant mechanism of the photoionization process provides access to many electronic states of a molecular ion.

Numerous investigations have been devoted to the SO<sub>2</sub><sup>+</sup> ion, including electron impact,<sup>4</sup> Penning ionization,<sup>5</sup> absorption spectroscopy,<sup>6</sup> photoelectron spectroscopy,<sup>7-13</sup> photoelectron-photoion coincidence spectroscopy,<sup>14,15</sup> photoelectron-fluorescence coincidence spectroscopy,<sup>16</sup> and photoionization mass spectrometry.<sup>17-21</sup> Surprisingly, the high resolution photoelectron spectrum for this ion is still not available, and the spectroscopy of the ion in its various electronic states remains poorly understood. Even the adiabatic ionization potentials in its different states are not completely consistent. In this paper, we report a high resolution He I photoelectron spectrum of SO<sub>2</sub> using a supersonic molecular beam.

The early He I photoelectron spectrum of SO<sub>2</sub><sup>+</sup> was taken by Turner *et al.*,<sup>7</sup> and by Eland and Danby.<sup>8</sup> Three bands were observed. One electronic state was assigned to the first band ( $\tilde{X}^2A_1$ ). Two states were assigned to the second band ( $\tilde{A}^2A_2$  and  $\tilde{B}^2B_2$ ) and the third band, respectively, though

Eland and Danby<sup>8</sup> pointed out that one single peak at 16.67 eV was observed in the third band of their spectrum and proposed that it could arise from a third state. Lloyd and Roberts<sup>9</sup> obtained a higher resolution spectrum of the third band and found that there were indeed three states ( $\tilde{C}^2B_2$ ,  $\tilde{D}^2A_1$ , and  $\tilde{E}^2B_1$ ) in the band, which was in agreement with theoretical predictions.<sup>22-25</sup> Potts<sup>11</sup> obtained low resolution He I (584 Å) and He II (303.8 Å) spectra of SeO<sub>2</sub> and SO<sub>2</sub>, trying to correlate the molecular orbitals in the two molecules. Recently, Holland, Parr, and Dehmer<sup>13</sup> measured the photoelectron asymmetry parameters and branching ratios for SO<sub>2</sub> in the 14–25 eV photon energy range by using synchrotron radiation.

The vibrational structure of the SO<sub>2</sub><sup>+</sup> PE spectrum is rather complicated, except for the first band, in which the vibrational structure was assigned to the  $\nu_2$  mode. In the second band, the vibrational structure of the state at higher IP was assigned to the  $\nu_2$  mode, but the vibrational structure of the state at lower IP was assigned in several ways; Turner *et al.*<sup>7</sup> assigned it by the  $\nu_2$  and  $\nu_3$  modes, while Eland and Danby<sup>8</sup> used the  $\nu_1$  and  $\nu_2$  modes. Cederbaum, Domcke, Niessen, and Kraemer<sup>26</sup> performed an *ab initio* many-body calculation on the vibrational structures for the first two bands ( $\tilde{X}^2A_1$ ,  $\tilde{A}^2A_2$ , and  $\tilde{B}^2B_2$  states), attempting to solve the difficult assignment problem. The  $\tilde{X}$  and  $\tilde{B}$  states seemed to be reproduced with the  $\nu_2$  mode only. They used the  $\nu_1$  and  $\nu_2$  modes to calculate the vibrational structure of the  $\tilde{A}^2A_2$  state, for which the result was less conclusive, because the experimental spectrum was not well resolved.<sup>7,8</sup> The third band of the spectrum is even more complicated, due to the heavy overlapping of the three electronic states and the spectral diffuseness at higher IP.

A molecular beam photoionization study of SO<sub>2</sub> was

reported by Erickson and Ng.<sup>20</sup> They obtained the photoionization efficiency (PIE) curves for SO<sub>2</sub><sup>+</sup>, SO<sup>+</sup>, and S<sup>+</sup>. They observed a complicated PIE curve for SO<sub>2</sub><sup>+</sup> in the 987–1006 Å range corresponding to the first band in the PE spectrum, from which they concluded that “the irregular spacing observed in the PIE curve rules out any simple assignment of the first photoelectron band to the ν<sub>2</sub> bending mode of SO<sub>2</sub><sup>+</sup>.”

The relaxation of the SO<sub>2</sub><sup>+</sup> ion has also been the topic of several research papers by different coincidence techniques.<sup>14–16</sup> An early photoelectron–photoion coincidence measurement showed that the dissociation of SO<sub>2</sub><sup>+</sup> ion in the third band could not be explained by either a statistical model or a model of direct dissociation.<sup>14</sup> A threshold photoelectron–photoion coincidence study revealed that S<sup>+</sup> formation occurred only in a very narrow energy range above the threshold.<sup>15</sup> A photoion–fluorescence photon coincidence study of radiative and dissociative relaxation processes in VUV photoexcited SO<sub>2</sub><sup>16</sup> showed that emission from electronic states lying above the dissociation threshold could be observed; that is, the radiative decay was competitive with the nonradiative decay or dissociation.

The C<sub>2v</sub> symmetry of SO<sub>2</sub><sup>27</sup> and the nature of the valence molecular orbitals of SO<sub>2</sub> are well established.<sup>22–25</sup> However, there have been very few theoretical studies on the SO<sub>2</sub><sup>+</sup> ion,<sup>22,26</sup> though there have been more experimental studies. We hope that the present work, by providing better experimental information, will inspire more sophisticated theoretical studies.

In what follows, we will give in Sec. II a brief account of the experimental technique. The results and discussion will be presented in Sec. III. A summary will be given in Sec. IV.

## II. EXPERIMENTAL

The molecular beam photoelectron spectrometer used for this study has been described in detail before.<sup>28</sup> Briefly, the supersonic SO<sub>2</sub> molecular beam, expanded from 200 Torr pure SO<sub>2</sub> (Matheson, Anhydrous grade, 99.98%) at room temperature through a 100 μm diam. nozzle and skimmed by a 0.9 mm diam. conical skimmer, was crossed perpendicularly by a photon beam from a rare gas discharge lamp. The electron energy analyzer consisted of a double electrostatic deflector operated at a pass energy of 1.0 eV, which sampled the photoelectrons at an angle of 90° with respect to both the photon beam and the molecular beam.

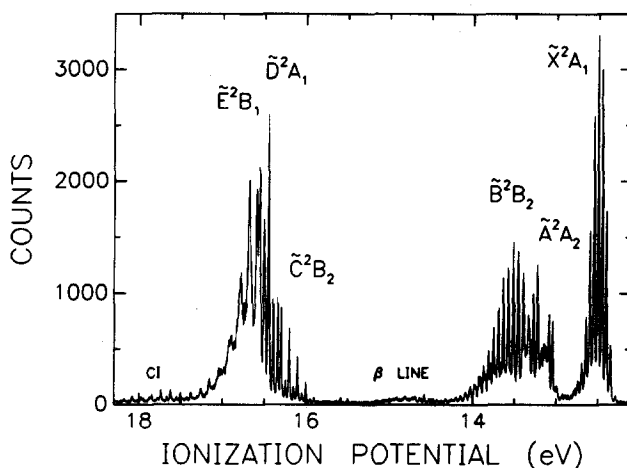


FIG. 1. The complete He I (584 Å) photoelectron spectrum of SO<sub>2</sub><sup>+</sup> measured with a resolution of 13 meV and a supersonic molecular beam of SO<sub>2</sub>.

The complete He I (584 Å) photoelectron spectrum of SO<sub>2</sub> was recorded with multichannel detection at a resolution of 13 meV FWHM, as measured on Ar<sup>+</sup> (<sup>2</sup>P<sub>3/2</sub>).

## III. RESULTS AND DISCUSSION

The complete He I photoelectron spectrum of SO<sub>2</sub> is displayed in Fig. 1, with state labelings shown. The improved resolution and rotational cooling permit the vibrational structure to be explicitly resolved. Besides the three main bands, two other weak bands at about 14.6 and 17.5 eV are also observed, with resolved vibrational structure. They were assigned as two satellite bands in a previous study.<sup>12</sup> An impurity peak of the X̄ N<sub>2</sub><sup>+</sup> (ν = 0) is observable in the spectrum at 15.6 eV. The B̄<sup>2</sup>Π<sub>u</sub> state of N<sub>2</sub><sup>+</sup> should be around 17.0 eV, but the intensity is negligible. Therefore, the SO<sub>2</sub><sup>+</sup> spectrum is not affected. In Table I, the adiabatic IPs of the first six states of SO<sub>2</sub><sup>+</sup> are given and compared with previous measurements where available, and the mean peak positions in all the states are listed in Tables II–VII. The present measurement of the adiabatic IP for the ground state is in excellent agreement with the value obtained from photoionization mass spectrometry reported by Erickson and Ng.<sup>20</sup> We note that the first peak in the ground state does not represent the adiabatic IP. As already pointed out by Erickson and Ng, it is a hot band transition. This was confirmed by changing the SO<sub>2</sub> stagnation pressure in the supersonic ex-

TABLE I. Adiabatic ionization potentials of the first seven electronic states of SO<sub>2</sub><sup>+</sup> (eV).

	X̄ <sup>2</sup> A <sub>1</sub>	Ā <sup>2</sup> A <sub>2</sub>	B̄ <sup>2</sup> B <sub>2</sub>	C̄ <sup>2</sup> B <sub>2</sub>	D̄ <sup>2</sup> A <sub>1</sub>	Ē <sup>2</sup> B <sub>1</sub>	F̄ <sup>2</sup> A <sub>1</sub>
a	12.349(3)	12.988(5)	13.338(4)	15.902(3)	16.339(3)	16.507(3)	
b	12.29	12.98		15.97	16.33		
c	12.30	13.01	13.24	15.986	16.326	(16.7)	
d				15.992	16.324	16.498	20.06
e	12.348(2)						

<sup>a</sup> This work.

<sup>b</sup> Turner *et al.* (Ref. 7).

<sup>c</sup> Eland and Danby (Ref. 8).

<sup>d</sup> Lloyd and Roberts (Ref. 9).

<sup>e</sup> Erickson and Ng (Ref. 20).

pansion. It can be seen from Table I that all the previous PES determinations of the adiabatic IP for the ground state were actually from the hot band. The onset of the  $\tilde{C}$  state shows another interesting case, where two more peaks are observed in the current spectrum. All previous measurements failed to observe these two peaks. This allows a new adiabatic IP to be determined for the  $\tilde{C}^2B_2$  state as 15.902(3) eV. This value is considerably lower than the previously measured values, as shown in Table I.

The vibrational assignment and discussions for the individual states are presented as follows.

### A. The $\tilde{X}^2A_1$ state

The separated spectrum of this state is plotted in Fig. 2. The previous PES studies<sup>7,8</sup> only partially resolved the vibrational structure, which was assigned to a single  $\nu_2$  progression. Erickson and Ng<sup>20</sup> observed a complicated PIE curve of SO<sub>2</sub>, and concluded that it was not possible to make a simple assignment of this band in the PE spectrum to the  $\nu_2$  bending mode only. In the present work, rotational cooling enables the vibrational structure to be fully resolved and allows the observed vibrational levels to be determined with improved accuracy. The vibrational structure in the present spectrum agrees with the assignment of a single  $\nu_2$  progression. The complicated PIE curve that Erickson and Ng observed may be due to autoionizations. The derived vibrational intervals,  $\Delta G(\nu_2 + 1/2)$ , are listed in Table II, and are plotted in Fig. 3 as a function of  $\nu_2$ . The vibrational spacings are regular up to  $\nu_2 = 7$ , with a positive anharmonicity. A least-squares fit over this range yields the following spectroscopic constants for  $\nu_2$ :  $\omega_e = 404 \pm 1$  cm<sup>-1</sup>,  $\omega_e x_e = 1.5 \pm 0.3$  cm<sup>-1</sup>. However, the spacings decrease drastically above  $\nu_2 = 7$ . This suggests that the photoionization transition reaches to the top of a potential barrier (to linearity) along the  $Q_2$  coordinate. The potential barrier may seriously perturb the vibrational levels around the barrier maximum. Essentially, a frequency halving should be observed far above the barrier maximum, as are the cases in

TABLE II. Ionization potentials (eV), vibrational frequencies (cm<sup>-1</sup>), and the assignment for the  $\tilde{X}^2A_1$  state of SO<sub>2</sub><sup>+</sup>.

IP	Assignment <sup>a</sup>	$\Delta G(\nu_2 + 1/2)$
12.2856(7) <sup>b</sup>	2 <sub>0</sub> <sup>1</sup> hot band	
12.3494(2)	0 0 0	515(3)
12.3995(2)	0 1 0	404.2(0.5) <sup>c</sup>
12.4493(2)	0 2 0	401.8(0.5) <sup>c</sup>
12.4985(2)	0 3 0	396.9(0.5) <sup>c</sup>
12.5474(2)	0 4 0	394.5(0.5) <sup>c</sup>
12.5960(2)	0 5 0	392.1(0.5) <sup>c</sup>
12.6443(2)	0 6 0	389.7(0.5) <sup>c</sup>
12.6923(2)	0 7 0	387.3(1.0) <sup>c</sup>
12.7382(4)	0 8 0	370.3(2)
12.7697(9)	0 9 0	254.1(8)
12.7878(10)	0 10 0	146.0(11)

<sup>a</sup> The assignment is labeled with the quantum numbers of  $\nu_1, \nu_2, \nu_3$ .

<sup>b</sup> The uncertainties of the absolute IPs are  $\pm 0.003$  eV. The smaller uncertainties quoted refer to the relative positions of the transitions, which are used to calculate the uncertainties for the vibrational splittings.

<sup>c</sup> Values used in the least-squares fitting.

H<sub>2</sub>S<sup>+</sup> ( $\tilde{A}^2A_1$ )<sup>29</sup> and NF<sub>3</sub><sup>+</sup> ground state.<sup>30</sup> An irregular vibrational structure will be observed as the transition approaches the barrier maximum. This can, in turn, allow an estimation of the barrier height. If we assume that the  $\nu_2 = 9$  level lies just above the barrier, we estimate the barrier height to be 0.42 eV (3400 cm<sup>-1</sup>) above the zero point energy. For the counterpart state in O<sub>3</sub><sup>+</sup>, Dyke, Golob, Jonathan, Morris, and Okuda<sup>31</sup> observed a complex vibrational structure at the beginning of the band. They estimated a barrier height to be 1880 cm<sup>-1</sup>. Although their assignment for the onset of the state has been questioned,<sup>20</sup> we believe that the assumption of a potential barrier is reasonable.

### B. The $\tilde{A}^2A_2$ and $\tilde{B}^2B_2$ states

An expanded spectrum of these two states is shown in Fig. 4. The overlapping of the two states and the lack of high resolution in the previous PES studies have led to controver-

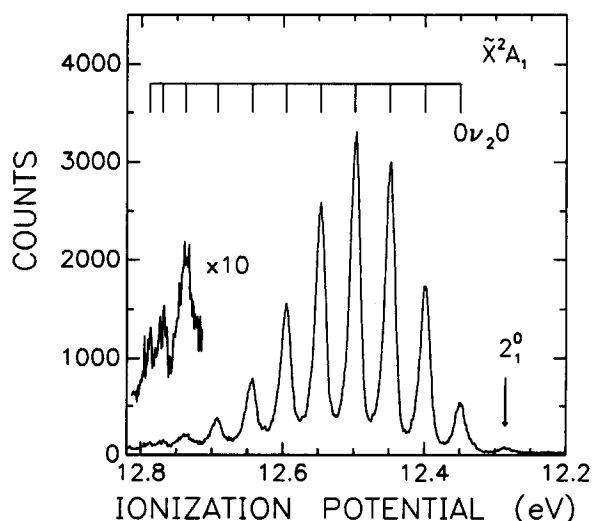


FIG. 2. The first band ( $\tilde{X}^2A_1$ , ground state) of the SO<sub>2</sub><sup>+</sup> He I photoelectron spectrum and the assignment.

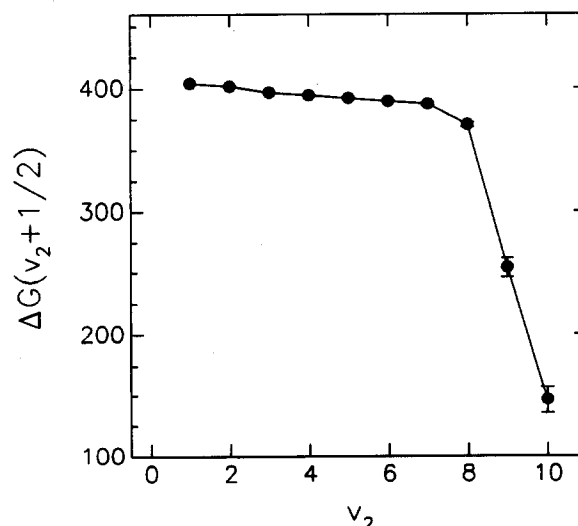


FIG. 3. The vibrational spacing  $\Delta G(\nu_2 + 1/2)$  of  $\nu_2$  in the  $\tilde{X}^2A_1$  state as a function of the vibrational quantum number  $\nu_2$ .

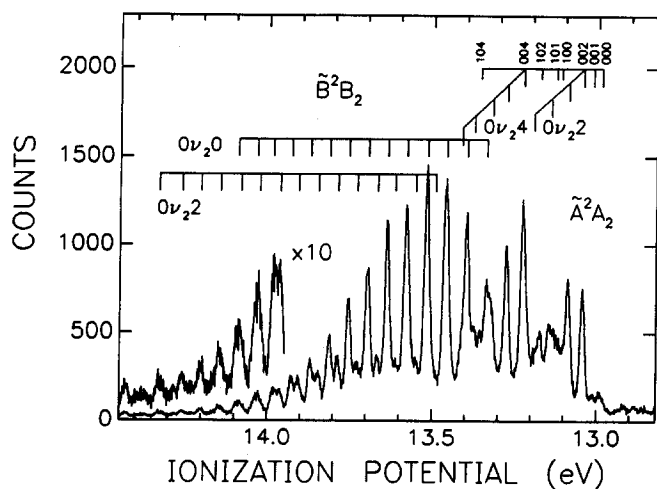


FIG. 4. The second band ( $\tilde{A}^2A_2$  and  $\tilde{B}^2B_2$  states) of the SO<sub>2</sub><sup>+</sup> He I photoelectron spectrum and the assignment.

sies about the adiabatic IPs and the vibrational assignment.<sup>7-13,22,26</sup> For the first state ( $\tilde{A}^2A_2$ ), Turner *et al.*<sup>7</sup> obtained an adiabatic IP of 12.98 eV, and Eland and Danby determined a value of 13.01 eV.<sup>8</sup> Turner *et al.* were not sure where the  $\tilde{B}^2B_2$  state started and did not determine the adiabatic IP, while Eland and Danby obtained an adiabatic IP of 13.24 eV by assuming that two components of the  $\tilde{B}^2B_2$  state overlapped with the  $\tilde{A}^2A_2$  state. The present spectrum has considerably higher resolution, which allows the IPs to be readily determined, as shown in Table I.

The  $\tilde{A}^2A_2$  state will be discussed first. This state was only partially resolved before, and no definite assignment is available. Turner *et al.*<sup>7</sup> used the combination of  $\nu_2$  and  $2\nu_3$  to assign the spectral features, and Eland and Danby<sup>8</sup> assigned them using  $\nu_1$  and  $\nu_2$ . Cederbaum *et al.*<sup>26</sup> did a many-body *ab initio* calculation on this difficult assignment problem. They used the vibrational constants reported by Eland

and Danby to model the vibrational structure. Though this approach produced an irregular vibrational progression, it could not be conclusive, because the experimental resolution was limited (0.035 eV). Two new features at the onset of this state are observed in the present spectrum. The spacing between these two weak peaks is 202(13) cm<sup>-1</sup>. The spacing between the second peak and the third sharp peak is 243(9) cm<sup>-1</sup>. Neither of these can belong to  $\nu_1$  or  $\nu_2$ . It is apparent that there are two  $\nu_2$  progressions starting at the third peak and at the most intense peak (i.e., at the peaks labeled 002 and 004 in Fig. 4). The spacing between these two progressions is 1467(2) cm<sup>-1</sup>. This is consistent with the assignment of  $2\nu_3$ . Turner *et al.*<sup>7</sup> did not resolve the first two weak peaks, so they assigned the spacing between the first peak and the most intense peak to be  $2\nu_3$  and obtained a  $2\nu_3$  value of 1860 cm<sup>-1</sup>. The  $\nu_3$  is an asymmetric vibrational mode, and only the even quantum levels are vibronically allowed.<sup>32</sup> The intensities of such a vibrational mode are normally very low, unless there is a big change of geometry or vibrational frequency in the ionic state. The unusually intense  $\nu_3$  excitation in the  $\tilde{A}^2A_2$  state here suggests that the  $\tilde{A}^2A_2$  state should have significantly distorted along the  $Q_3$  coordinate. If we take into account the two newly resolved features of the state, which we assign to two early components of the  $\nu_3$  vibration, we find that the  $\nu_3$  mode has rather erratic vibrational levels, suggesting that a potential barrier may exist along the  $Q_3$  coordinate. This potential barrier separates two equivalent unsymmetric SO<sub>2</sub><sup>+</sup> ions with the two S-O bonds being unequal (*C<sub>s</sub>* symmetry). The unusually small spacings of  $\nu_3$  at the beginning of the progression are consistent with being around the barrier maximum. Assuming that only the first level is below the barrier maximum, we estimate the barrier height to be less than 202 cm<sup>-1</sup>. A similar case was observed in the electronic absorption spectrum of SO<sub>2</sub> for the transition  $\tilde{C}^1B_2 \leftarrow \tilde{A}^1A_1 [b_1(\Pi^*)] \leftarrow 1a_2(\Pi)$ , where an electron was excited from the  $1a_2$  orbital to the  $b_1$  antibonding orbital.<sup>33</sup> The spectrum was very complicated

TABLE III. Ionization potentials (eV), vibrational frequencies (cm<sup>-1</sup>), and the assignment for the  $\tilde{A}^2A_2$  state of SO<sub>2</sub><sup>+</sup>.

IP	Assignment <sup>a</sup>	$\nu_1$	$\Delta G(\nu_2 + 1/2)$	$\nu_3$
12.9884(21) <sup>b</sup>	0 0 0			
13.0134(21)	0 0 1			202(13)
13.0435(6)	0 0 2			243(9)
13.0873(10)	0 1 2		353(7)	
13.1100(82)	1 0 0	981(60)		
13.1255(98)	1 0 1	904(71)		
13.1436(33)	0 2 2		452(15)	
13.1730(19)	1 0 2	1045(10)		
13.1894(80)	0 3 2		370(60)	
13.2253(6)	0 0 4			1466.8(1.4) <sup>c</sup>
13.2749(6)	0 1 4		400.2(1.6)	
13.3236(23)	0 2 4		393(18)	
13.3569(8)	1 0 4	1062(5)		
13.3730(13)	0 3 4		399(9)	
13.4120(31)	0 4 4		315(12)	

<sup>a</sup> The assignment is labeled with the quantum numbers of  $\nu_1$ ,  $\nu_2$ ,  $\nu_3$ .

<sup>b</sup> See footnote b in Table II.

<sup>c</sup>  $2\nu_3$  value.

TABLE IV. Ionization potentials (eV), vibrational frequencies (cm<sup>-1</sup>), and the assignment for the  $\tilde{B}^2B_2$  state of SO<sub>2</sub><sup>+</sup>.

IP	Assignment <sup>a</sup>	$\Delta G(v_2 + 1/2)$	$2\nu_3$
13.3384(12) <sup>b</sup>	0 0 0		
13.3960(7)	0 1 0	465(9)	
13.4578(6)	0 2 0	499(4)	
13.4900(50)	0 0 2		1223(13)
13.5169(7)	0 3 0	477(1)	
13.5503(10)	0 1 2		1245(8)
13.5775(6)	0 4 0	489(1)	
13.6131(31)	0 2 2		1253(24)
13.6360(6)	0 5 0	472(2)	
13.6657(7)	0 3 2		1201(3)
13.6952(6)	0 6 0	478(2)	
13.7279(8)	0 4 2		1213(5)
13.7538(6)	0 7 0	473(2)	
13.7856(7)	0 5 2		1207(5)
13.8113(6)	0 8 0	464(2)	
13.8459(9)	0 6 2		1216(6)
13.8700(7)	0 9 0	474(2)	
13.9059(9)	0 7 2		1227(7)
13.9277(8)	0 10 0	466(2)	
13.9611(14)	0 8 2		1209(10)
13.9826(15)	0 11 0	443(12)	
14.0232(34)	0 9 2		1236(15)
14.0309(20)	0 12 0	390(20) <sup>c</sup>	
14.0800(140)	0 10 2		1229(43)
14.0891(150)	0 13 0	470(45) <sup>c</sup>	

<sup>a</sup> The assignment is labeled with the quantum numbers of  $\nu_1$ ,  $\nu_2$ ,  $\nu_3$ .

<sup>b</sup> See footnote b in Table II.

<sup>c</sup> Values not used in the least-squares fitting.

and the interpretation involved assuming a double well potential along the  $Q_3$  coordinate. Therefore, the equilibrium geometry of SO<sub>2</sub> in the  $\tilde{C}^1B_2$  state was unsymmetric. A subsequent theoretical treatment<sup>34</sup> yielded the barrier height to be 141 cm<sup>-1</sup> and the equilibrium values of the short and long S–O bonds to be 1.491 and 1.639 Å, respectively (compared with 1.4321 Å for the SO<sub>2</sub> ground state<sup>35</sup>). The calculated energy levels for the  $\nu_3$  mode were  $1\nu_3 = 211$  cm<sup>-1</sup>,  $2\nu_3 = 562$  cm<sup>-1</sup>,  $3\nu_3 = 891$  cm<sup>-1</sup>, and  $4\nu_3 = 1249$  cm<sup>-1</sup>, which are comparable to the  $\nu_3$  energy levels for SO<sub>2</sub><sup>+</sup> ( $\tilde{B}^2A_2$ ) observed in our spectrum, as seen from Table III. As a matter of fact, Jaffe<sup>36</sup> has treated the nonrigid SO<sub>2</sub> molecule in the  $\tilde{C}^1B_2$  state by classical mechanics and reassigned the observed vibrational structure of the  $\tilde{C}^1B_2 \leftarrow \tilde{X}^1A_1$  electronic transition by a set of local modes and normal modes. A more recent study by Innes<sup>37</sup> has tried to establish the origin of the unequal bond lengths in the  $\tilde{C}^1B_2$  state of SO<sub>2</sub>. The  $\tilde{C}^1B_2$  state of SO<sub>2</sub> and the  $\tilde{A}^2A_2$  state of SO<sub>2</sub><sup>+</sup> should have similar properties, since both involve removing an electron from the same orbital ( $1a_2$ ).

The transition to the  $\nu_3 = 1$  level in the  $\tilde{A}^2A_2$  state is a vibronically forbidden transition without any vibronic interaction.<sup>32</sup> The observation of such a transition indicates some degree of vibronic interaction in the  $\tilde{A}$  state of SO<sub>2</sub><sup>+</sup>. Indeed, Innes<sup>37</sup> has found that the asymmetric SO<sub>2</sub> in the  $\tilde{C}^1B_2$  state originates from the vibronic coupling between the  $\tilde{C}^1B_2$  state and a higher  $^1A_1$  state. The same argument may apply to the asymmetric SO<sub>2</sub><sup>+</sup> in the  $\tilde{A}^2A_2$  state, since the vibronic effect is not negligible in this state.

The complete assignment for the  $\tilde{A}^2A_2$  state is shown in Fig. 4. The IPs and the vibrational intervals are listed in Table III. The transition to  $\nu_3 = 3$  may also contribute to the broad feature at 13.11 eV.

The assignment for the  $\tilde{B}^2B_2$  state is reasonably straightforward. Both Turner *et al.*<sup>7</sup> and Eland and Danby<sup>8</sup> assigned the vibrational structure to a single  $\nu_2$  progression. The main features of the present spectrum is in agreement with the assignment to the  $\nu_2$  mode, except that we have resolved another new progression with smaller intensity. The derived  $G(v_2 + 1/2)$  values for the main progression are listed in Table IV. A least-squares fitting of  $G(v_2 + 1/2)$  vs  $v_2$  yields the following spectroscopic constants:  $\omega_e = 489 \pm 5$  cm<sup>-1</sup>,  $\omega_e\chi_e = 2 \pm 1$  cm<sup>-1</sup>. However, if we plot the  $\Delta G(v_2 + 1/2)$  vs  $v_2$  in an expanded scale, we can see, from Fig. 5, that the vibrational intervals do not decrease linearly as a function of  $v_2$  within the experimental uncertainty.

The new progression with lower intensity is assigned to another  $\nu_2$  progression in combination with either  $\nu_1$  or  $\nu_3$ . The difference between this progression and the main progression is 1223 cm<sup>-1</sup>, which cannot be  $\nu_1$  (1151.3 cm<sup>-1</sup> for SO<sub>2</sub><sup>35</sup>). We assign it to  $2\nu_3$  since  $1\nu_3$  is vibronically forbidden.

The fact that the  $\nu_3$  mode is active in the  $\tilde{B}^2B_2$  state suggests that the  $\tilde{B}^2B_2$  state is also somehow distorted along the  $Q_3$  coordinate. Since the  $\tilde{B}^2B_2$  and  $\tilde{A}^2A_2$  states are from ionizing  $5b_2$  and  $1a_2$  orbitals, both of which originate from the S *d*-orbital bonding, there is no surprise that the two

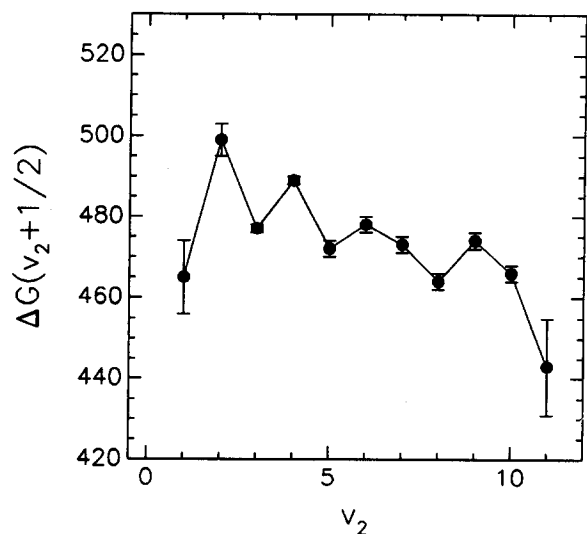


FIG. 5. The vibrational spacing  $\Delta G(v_2 + 1/2)$ , of  $v_2$  in the  $\tilde{B}^2B_2$  state as a function of the vibrational quantum number  $v_2$ .

states should have some similar characteristics. They are both displaced along the  $Q_2$  and  $Q_3$  coordinates with respect to the neutral ground state, and, therefore, both have very different geometries from the ground state. The  $\tilde{A}^2A_2$  state is displaced more along the  $Q_3$  coordinate, and the  $\tilde{B}^2B_2$  state is displaced more along the  $Q_2$  coordinate. This is consistent with the fact that the major vibrational progression is  $\nu_3$  for the  $\tilde{A}^2A_2$  state, and  $\nu_2$  for the  $\tilde{B}^2B_2$  state. However, it is not clear from the current spectrum whether the  $\tilde{B}^2B_2$  state also has an asymmetric equilibrium geometry like the  $\tilde{A}^2A_2$  state. From the fact that the  $\nu_2$  mode in the  $\tilde{B}^2B_2$  state has an abnormal spacing dependence with  $v_2$ , we conclude that the  $\nu_3$  mode couples with the  $\nu_2$  mode in the  $\tilde{B}^2B_2$  state so that the  $\nu_2$  mode differs from a normal anharmonic oscillator, as shown in Fig. 5.

### C. The $\tilde{C}^2B_2$ , $\tilde{D}^2A_1$ , and $\tilde{E}^2B_1$ states

The spectrum of these states is shown in Fig. 6. The overlapping of the three states and the diffuseness at the high IP side have made the assignment more difficult. In the early PES studies, some inconsistencies arose about the number of states in the band. Turner *et al.*<sup>7</sup> and Eland and Danby<sup>8</sup> assigned only two states in their early studies. It was Lloyd and Roberts<sup>9</sup> who first assigned the third state from a better resolved spectrum. Their assignment was  $\tilde{C}^2B_2$ ,  $\tilde{D}^2A_1$ ,  $\tilde{E}^2B_1$ , obtained by comparing their experimental evidence with Hillier and Saunders's *ab initio* SCFMO calculation.<sup>22</sup>

The higher sensitivity of the present experiment allows two new features to be observed at the onset of the  $\tilde{C}$  state. These two weak peaks have eluded previous investigations. We may conservatively regard the first peak as the adiabatic transition to the  $\tilde{C}$  state. This yields an adiabatic IP of 15.902(3) eV for the  $\tilde{C}$  state. It is, however, possible that the true adiabatic transition is too weak to be observed even by this experiment. Then, the presently reported value should be regarded as an upper bound on the adiabatic IP.

Even having lower resolution compared with this experiment, Lloyd and Roberts<sup>9</sup> could still assign all the major

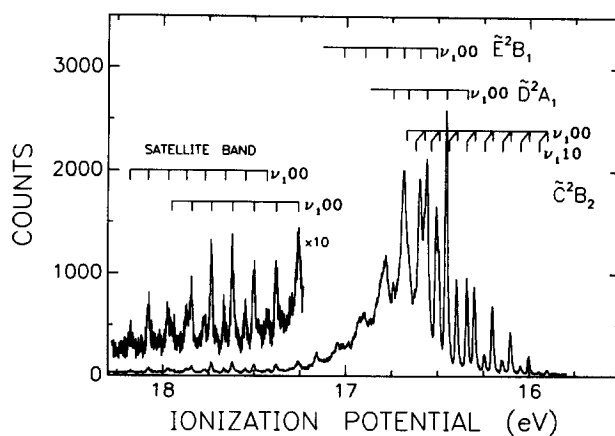


FIG. 6. The satellite band and the third band ( $\tilde{C}^2B_2$ ,  $\tilde{D}^2A_1$ , and  $\tilde{E}^2B_1$  states) of the SO<sub>2</sub><sup>+</sup> He I photoelectron spectrum and the assignment.

spectral features. Their assignment agrees with our assignment in Fig. 6. For the  $\tilde{C}^2B_2$  state, both  $\nu_1$  and  $\nu_2$  modes are excited. The  $\nu_1$  mode is excited much more than the  $\nu_2$  mode and comprises the major vibrational progression, as shown in Fig. 6. We can observe  $\nu_1$  up to  $\nu_1 = 8$ , which we believe is the full Franck-Condon region of the  $\tilde{C}^2B_2$  state, for reasons we will discuss later. The derived vibrational intervals,  $\Delta G(v_1 + 1/2)$ , are shown in Table V. A least-squares fit of  $\Delta G(v_1 + 1/2)$  vs  $v_1$  yields the following spectroscopic constants for  $\nu_1$ :  $\omega_e = 816 \pm 3$  cm<sup>-1</sup>,  $\omega_e \chi_e = 3 \pm 0.5$  cm<sup>-1</sup>. The average  $\nu_2$  value is  $365 \pm 3$  cm<sup>-1</sup>. The  $\tilde{D}^2A_1$  and  $\tilde{E}^2B_1$  states are assigned with the  $\nu_1$  mode only. Although Lloyd and Roberts have assigned all the spectral features, we still find that it is difficult to make a thorough assignment, and to find the spectroscopic constants for these two states by the routine least-squares fitting method, because the spectrum becomes rather diffuse toward the high energy side. The vibrational spacings which can be determined are listed in Table VI.

The broadened spectrum indicates that fast dynamical processes occur in the excited ionic states. The dissociation limits of SO<sub>2</sub><sup>+</sup> to form SO<sup>+</sup> + O and S<sup>+</sup> + O<sub>2</sub> in their ground states are 15.95 and 16.23 eV, respectively. These are the only two dissociation channels which can occur in these three states. Three accounts have been given of the dissociation mechanisms for the ion.<sup>14-16</sup> From their threshold photoelectron-photoion coincidence experiment, Weiss, Hsieh, and Meisels<sup>15</sup> observed that S<sup>+</sup> was only formed in a very narrow energy range between 16.334–16.674 eV and that SO<sub>2</sub><sup>+</sup> became fully predissociated above about 16.67 eV. They explained the formation of SO<sup>+</sup> and S<sup>+</sup> by using a vibrational predissociation model in the  $\tilde{C}^2B_2$  state. Dujardin and Leach<sup>16</sup> made a photoion-fluorescence photon coincidence measurement and concluded that S<sup>+</sup> could not be formed in the  $\tilde{C}^2B_2$  state, but must come from a higher state. They observed fluorescence in coincidence with SO<sub>2</sub><sup>+</sup> in the third band with a small quantum yield.

It has been shown that a high resolution photoelectron spectrum can provide useful dynamical information about the molecular ion, through the correlation functions obtained by Fourier transformations of the individual elec-

TABLE V. Ionization potentials (eV), vibrational frequencies (cm<sup>-1</sup>), and the assignment for the  $\tilde{C}^2B_2$  state of SO<sub>2</sub><sup>+</sup>.

IP	Assignment <sup>a</sup>	$\Delta G(v_1 + 1/2)$	$\nu_2$
15.9020(9) <sup>b</sup>	0 0 0		
15.9480(13)	0 1 0		371(10)
16.0012(8)	1 0 0	800(4)	
16.0468(8)	1 1 0		368(4)
16.1011(8)	2 0 0	806(2)	
16.1460(8)	2 1 0		362(2)
16.1999(8)	3 0 0	797(2)	
16.2441(8)	3 1 0		357(2)
16.2983(7)	4 0 0	794(1)	
16.3956(7)	5 0 0	785(1)	
16.4922(10)	6 0 0	779(5)	
16.5860(80)	7 0 0	757(20) <sup>c</sup>	
16.6240(50)	7 1 0		310(46)

<sup>a</sup>The assignment is labeled with the quantum numbers of  $\nu_1, \nu_2, \nu_3$ .

<sup>b</sup>See footnote b in Table II.

<sup>c</sup>Value not used in the least-squares fitting.

tronic bands in the photoelectron spectrum.<sup>3(b),38,39</sup> In the case of the third band of SO<sub>2</sub><sup>+</sup>, the strong overlapping of the three electronic states precludes deriving useful correlation functions. However, the dynamical information that a photoelectron spectrum carries does not depend on the correlation functions. In high resolution PES, the instrumental function limits the time scale on which the ultrafast dynamics can be measured. With an instrumental resolution of 13 meV, we obtain an upper limit of 51 fs for this time scale from the time-energy uncertainty principle. In other words, any state with a lifetime shorter than 51 fs will broaden the spectrum. Therefore, the spectral diffuseness signals the presence of ultrafast processes, from which the dynamics can be inferred.

In the third band of SO<sub>2</sub><sup>+</sup> the spectrum becomes considerably broadened above about 16.7 eV, which means the ultrafast dissociation starts around 16.7 eV. The spectrum below 16.7 eV essentially represents the instrumental resolution, indicating that the states below 16.7 eV have lifetimes longer than 51 fs, that is, the  $\tilde{C}$  state is relatively stable as it covers this whole range. This is consistent with the ob-

servation of fluorescence from this region of the spectrum, which gave a lifetime of less than 10 ns.<sup>16</sup> This also agrees with Weiss *et al.*'s experiment,<sup>15</sup> which shows that SO<sub>2</sub><sup>+</sup> is completely predissociated above 16.67 eV. However, it has been observed that the ion does dissociate from the  $\tilde{C}^2B_2$  state, and various interpretations<sup>14-16</sup> have been given to the dissociation mechanisms. The ion can not directly dissociate through this state, since that would require the  $\tilde{C}^2B_2$  state to have a very shallow potential well.<sup>16</sup> Therefore, the dissociations from the  $\tilde{C}$  state have to proceed through the lower lying states, by electronic predissociations. Because SO<sub>2</sub><sup>+</sup> is a small molecule and there is a big  $\tilde{C}-\tilde{B}$  state energy gap, these predissociations are unfavored. It is these unfavored processes that actually lengthen the lifetime of the state so that the fluorescence is competitive with the predissociations.

The combination of the SO<sup>+</sup> ( $\tilde{X}^2\Pi$ ) + O(<sup>3</sup>P<sub>g</sub>) product states can lead to 12 states in the C<sub>s</sub> molecular symmetry. These 12 states [3(<sup>2,4</sup>A') and 3(<sup>2,4</sup>A'')] can correlate, in the C<sub>2v</sub> point group, with all four possible species A<sub>1</sub>, A<sub>2</sub>, B<sub>1</sub>, and B<sub>2</sub>. We propose that the formation of SO<sup>+</sup> + O occurs through a predissociation by either the  $\tilde{A}^2A_2$  state or the

TABLE VI. Ionization potentials (eV), vibrational frequencies (cm<sup>-1</sup>) and the assignment for the  $\tilde{D}^2A_1$  and  $\tilde{E}^2B_1$  states of SO<sub>2</sub><sup>+</sup>.

IP	Assignment <sup>a</sup>	$\Delta G(v_1 + 1/2)^b$	$\Delta G(v_1 + 1/2)^c$
16.3393(7) <sup>b,d</sup>	0 0 0		
16.4523(7) <sup>b</sup>	1 0 0	912(0.7)	
16.5074(8) <sup>c</sup>	0 0 0		
16.5601(8) <sup>b</sup>	2 0 0	869(1)	
16.5949(9) <sup>c</sup>	1 0 0		706(4)
16.6580(60) <sup>b</sup>	3 0 0	790(25)	
16.6858(20) <sup>c</sup>	2 0 0		
16.7415(10) <sup>b</sup>	4 0 0		
16.7813(30) <sup>c</sup>	3 0 0		

<sup>a</sup>The assignment is labeled with the quantum numbers of  $\nu_1, \nu_2, \nu_3$ .

<sup>b</sup>For the  $\tilde{D}^2A_1$  state.

<sup>c</sup>For the  $\tilde{E}^2B_1$  state.

<sup>d</sup>See footnote b in Table II.

TABLE VII. Ionization potentials (eV), vibrational frequencies (cm<sup>-1</sup>), and the assignment for the satellite band.

IP	Assignment <sup>a</sup>	$\Delta G(\nu_1 + 1/2)^b$	$\Delta G(\nu_1 + 1/2)^c$
17.2575(9) <sup>b,d</sup>	0 0 0		
17.3783(9) <sup>b</sup>	1 0 0	975(10)	
17.4261(20) <sup>c</sup>	0 0 0		
17.5006(9) <sup>b</sup>	2 0 0	987(5)	
17.5478(10) <sup>c</sup>	1 0 0		982(18)
17.6184(8) <sup>b</sup>	3 0 0	950(5)	
17.6648(10) <sup>c</sup>	2 0 0		944(10)
17.7342(8) <sup>b</sup>	4 0 0	934(14)	
17.7725(10) <sup>c</sup>	3 0 0		869(10)
17.8429(10) <sup>b</sup>	5 0 0	877(7)	
17.8684(20) <sup>c</sup>	4 0 0		774(13)
17.9472(23) <sup>b</sup>	6 0 0	842(19)	
17.9718(13) <sup>c</sup>	5 0 0		834(14)
18.076(10) <sup>c</sup>	6 0 0		840(10)
18.176(20) <sup>c</sup>	7 0 0		808(17)

<sup>a</sup>The assignment is labeled with the quantum numbers of  $\nu_1, \nu_2, \nu_3$ .

<sup>b</sup>For progression 1.

<sup>c</sup>For progression 2.

<sup>d</sup>See footnote b in Table II.

$\bar{B}^2B_2$  state, both of which show distortions along the direction of  $Q_3$  favorable to the asymmetric dissociation. However, in the formation of  $S^+ + O_2$ , the whole molecular symmetry ( $C_{2v}$ ) is retained, and combination of the products in their ground states yields states of  ${}^{6,4,2}B_2$  symmetry. Therefore, the dissociation to  $S^+ + O_2$  can be through a predissociation of the  $\bar{C}^2B_2$  state by the  $\bar{B}^2B_2$  state, for which the  $\nu_2$  mode is observed to be strongly excited favorable the dissociation channel to  $S^+ + O_2$ . This is consistent with Weiss *et al.*'s suggestion that  $S^+$  is produced entirely from the  $\bar{C}^1B_2$  state.<sup>15</sup> Therefore, this would explain why  $S^+$  was only observed in a narrow energy range, since it is out of the Franck-Condon region of the  $\bar{C}$  state above 16.7 eV.

The  $\bar{D}$  and  $\bar{E}$  states are responsible for the fast dissociations above 16.7 eV, as evidenced by the spectral diffuseness. In the absence of any theoretical calculation, the only dissociation pathway we can suggest would be predissociations through the  $\bar{C}^2B_2$  state, since the spectral feature precludes any direct dissociation model.

#### D. The satellite band

Two weak bands which occur at about 14.6 and 17.5 eV were interpreted by Kimura *et al.* as two satellite bands.<sup>12</sup> Vibrational structure is resolved in the current spectrum, as seen from Figs. 1 and 6. It turns out that the band at 14.6 eV is the He I  $\beta$  line (537 Å) spectrum of the third band. The band at 17.5 eV is a satellite band, because the  $\bar{F}^2A_1$  state is at 20.06 eV<sup>9,11</sup> and the  $\beta$  line spectrum would occur at a higher energy. Satellite bands are well known in the photoionization of the inner shell electrons for molecules containing the first and second row elements,<sup>40</sup> and satellite bands in the valence region have been observed in molecules containing the third row elements.<sup>41</sup> The band we observed consists of two  $\nu_1$  vibrational progressions which may be two components of a spin-orbit split state. The energies and spacings are listed in Table VII. Autoionization was proposed for this

band,<sup>11</sup> but the sharp features of the vibrational structure exclude this possibility.

#### IV. SUMMARY

High resolution PES study of SO<sub>2</sub> using a supersonic molecular beam allows us to study the first six states of SO<sub>2</sub><sup>+</sup> in greater detail, in addition to obtain improved IPs. A potential barrier was found for the  $\bar{X}^2A_1$  state along the  $Q_2$  coordinate. The barrier height for the  $\bar{X}^2A_1$  state was estimated to be 0.42 eV (3400 cm<sup>-1</sup>). For the  $\bar{A}^2A_2$  state, we observed unusual vibrational structure, which was explained by the principal excitation of the  $\nu_3$  mode upon photoionization and the presence of a potential barrier along the  $Q_3$  coordinate. The ion in this state possesses an asymmetric equilibrium geometry. The barrier height for the  $\bar{A}$  state was estimated to be less than 220 cm<sup>-1</sup>. A new progression was resolved in the  $\bar{B}^2B_2$  state, which was assigned to be the combination of  $\nu_2$  with  $2\nu_3$ . The  $\bar{A}$  and  $\bar{B}$  states were found to have some similar characteristics. Two new features were observed for the  $\bar{C}^2B_2$  state, which allowed a new adiabatic IP to be determined for the  $\bar{C}$  state. The decay of the  $\bar{C}$  state was discussed and predissociations through the lower lying states are suggested. The spectrum above 16.7 eV is much broadened, suggesting that rapid dissociations occur from the  $\bar{D}^2A_1$  and  $\bar{E}^2B_1$  states. Predissociations by the  $\bar{C}^2B_2$  state were proposed.

A weak band at about 14.6 eV, which had been assigned as a satellite band, was found to be a He I  $\beta$  line (537 Å) spectrum of the third band. A satellite band at about 17.5 eV with resolved vibrational structure was observed.

#### ACKNOWLEDGMENTS

This work was supported by the Director, Office of Energy Research, Office of Basic Energy Sciences, Chemical



Science Division of the U.S. Department of Energy under Contract No. DE-ACO3-76SF00098.

- <sup>1</sup>See for example, (a) *Molecular Ions: Geometric and Electronic Structures*, edited by J. Berkowitz and K. O. Groenfeld (Plenum, New York, 1983); (b) A special issue of *J. Chim. Phys.* **77**, 585-777 (1980); (c) *Molecular Ions: Spectroscopy, Structure, and Chemistry*, edited by T. A. Miller and V. E. Bondybey (North-Holland, Amsterdam, 1983).
- <sup>2</sup>J. E. Pollard, D. J. Trevor, J. E. Reutt, Y. T. Lee, and D. A. Shirley, *J. Chem. Phys.* **77**, 34 (1982).
- <sup>3</sup>(a) J. E. Pollard, D. J. Trevor, J. E. Reutt, Y. T. Lee, and D. A. Shirley, *J. Chem. Phys.* **81**, 5302 (1984); (b) J. E. Reutt, L. S. Wang, Y. T. Lee, and D. A. Shirley, *ibid.* **85**, 6928 (1986).
- <sup>4</sup>(a) H. D. Smyth and D. W. Mueller, *Phys. Rev.* **43**, 121 (1933); (b) R. M. Reese, V. H. Dibeler, and J. L. Franklin, *J. Chem. Phys.* **29**, 880 (1958); (c) R. Hagemann, *C. R. Acad. Sci.* **255**, 1102 (1962); (d) R. Botter, R. Hagemann, G. Nief, and E. Roth, *Advances in Mass Spectrometry* (The Institute of Petroleum, London, 1966), Vol. 3, p. 951.
- <sup>5</sup>C. E. Brion and D. S. C. Yee, *J. Electron Spectrosc. Relat. Phenom.* **12**, 77 (1977).
- <sup>6</sup>(a) W. C. Price and D. M. Simpson, *Proc. R. Soc. London Ser. A* **165**, 272 (1938); (b) D. Golomb, K. Watanabe, and F. F. Marmo, *J. Chem. Phys.* **36**, 958 (1962).
- <sup>7</sup>D. W. Turner, C. Baker, A. D. Baker, and C. R. Brundle, *Molecular Photoelectron Spectroscopy* (Wiley-Interscience, London, 1970).
- <sup>8</sup>J. H. D. Eland and C. J. Danby, *Int. J. Mass Spectrom. Ion Phys.* **1**, 111 (1968).
- <sup>9</sup>D. R. Lloyd and P. J. Roberts, *Mol. Phys.* **26**, 225 (1973).
- <sup>10</sup>H. Bock, B. Solouki, P. Rosmus, R. Steudel, and W. Schultheis, *Angew. Chem.* **85**, 987 (1973).
- <sup>11</sup>A. W. Potts, *J. Electron Spectrosc. Relat. Phenom.* **11**, 157 (1977).
- <sup>12</sup>K. Kimura, S. Katsumata, Y. Achiba, T. Yamazaki, and S. Iwata, *Handbook of He I Photoelectron Spectra of Fundamental Organic Molecules* (Japan Scientific Societies, Tokyo, 1981).
- <sup>13</sup>D. M. P. Holland, A. C. Parr, and J. L. Dehmer, *J. Electron Spectrosc. Relat. Phenom.* **32**, 237 (1983).
- <sup>14</sup>B. Brehm, J. H. D. Eland, R. Frey, and A. Küstler, *Int. J. Mass Spectrom. Ion Phys.* **12**, 197 (1973).
- <sup>15</sup>M. J. Weiss, T. C. Hsieh, and G. G. Meisels, *J. Chem. Phys.* **71**, 567 (1979).
- <sup>16</sup>C. Dujardin and S. Leach, *J. Chem. Phys.* **76**, 2521 (1981).
- <sup>17</sup>E. C. Y. Inn, *Phys. Rev.* **91**, 1194 (1953).
- <sup>18</sup>K. Watanabe, *J. Chem. Phys.* **26**, 542 (1957).
- <sup>19</sup>V. H. Dibeler and S. K. Liston, *J. Chem. Phys.* **49**, 482 (1968).
- <sup>20</sup>J. Erickson and C. Y. Ng, *J. Chem. Phys.* **75**, 1650 (1981).
- <sup>21</sup>C. Y. R. Wu and C. Y. Ng, *J. Chem. Phys.* **76**, 4406 (1982).
- <sup>22</sup>I. H. Hillier and V. R. Saunders, *Mol. Phys.* **22**, 193 (1971).
- <sup>23</sup>S. Rothenberg and H. F. Schaefer III, *J. Chem. Phys.* **53**, 3014 (1970).
- <sup>24</sup>J. G. Norman, Jr., *Mol. Phys.* **31**, 1191 (1976).
- <sup>25</sup>L. Noodleman and K. A. R. Mitchell, *Inorg. Chem.* **17**, 2709 (1978).
- <sup>26</sup>L. S. Cederbaum, W. Domcke, W. V. Niessen, and W. P. Kraemer, *Mol. Phys.* **34**, 381 (1977).
- <sup>27</sup>G. Herzberg, *Infrared and Raman Spectra of Polyatomic Molecules* (Van Nostrand Reinhold, New York, 1945), p. 285.
- <sup>28</sup>J. E. Pollard, D. J. Trevor, Y. T. Lee, and D. A. Shirley, *Rev. Sci. Instrum.* **52**, 1837 (1981).
- <sup>29</sup>L. Karlsson, L. Mattsson, R. Jadrny, T. Bergmark, and K. Siegbahn, *Phys. Scr.* **13**, 229 (1976).
- <sup>30</sup>J. Berkowitz and J. P. Greene, *J. Chem. Phys.* **81**, 3383 (1984).
- <sup>31</sup>J. M. Dyke, L. Golob, N. Jonathan, A. Morris, and M. Okuda, *J. Chem. Soc. Faraday Trans. 2* **70**, 1828 (1974).
- <sup>32</sup>J. R. Rabalais, *Principle of Ultraviolet Photoelectron Spectroscopy* (Wiley, New York, 1977), p. 70.
- <sup>33</sup>(a) V. T. Jones and J. B. Coon, *J. Mol. Spectrosc.* **47**, 45 (1973). (b) J. C. D. Brand, P. H. Chiu, and A. R. Hoy, *ibid.* **69**, 43 (1976).
- <sup>34</sup>A. R. Hoy and J. C. D. Brand, *Mol. Phys.* **36**, 1409 (1978).
- <sup>35</sup>G. Herzberg, *Electronic Spectra and Electronic Structures of Polyatomic Molecules* (Litton Educational, New York, 1966), p. 605.
- <sup>36</sup>C. Jaffe, *J. Chem. Phys.* **81**, 616 (1984).
- <sup>37</sup>K. K. Innes, *J. Mol. Spectrosc.* **120**, 1 (1986).
- <sup>38</sup>(a) J. E. Pollard, D. J. Trevor, J. E. Reutt, Y. T. Lee, and D. A. Shirley, *J. Chem. Phys.* **81**, 5302 (1984); (b) R. McDiarmid, *J. Phys. Chem.* **84**, 64 (1980).
- <sup>39</sup>A. J. Lorquet, J. C. Lorquet, J. Delwiche, and M. T. Hubin-Franskin, *J. Chem. Phys.* **76**, 4692 (1982).
- <sup>40</sup>A. W. Potts and T. A. Williams, *J. Electron Spectrosc. Relat. Phenom.* **3**, 3 (1974).
- <sup>41</sup>I. Reineck, B. Wannberg, H. Veenhuizen, C. Nohre, R. Maripuu, K. E. Nozell, L. Mattsson, L. Karlsson, and K. Siegbahn, *J. Electron Spectrosc. Relat. Phenom.* **34**, 235 (1984).